Dear Editor,

thank you very much for sending us the reports of the two Referees. We are grateful to the Referees for their careful, positive and constructive reports that helped us improving our manuscript. We have revised the manuscript complying with the requests of both Referees, and we have replaced the arXiv manuscript with the revised one. Our detailed point-by-point response to the Referees has been uploaded.

In view of the already positive reports of both Referees and of the substantial improvements that we have implemented in response to their comments, we are confident that this revised version of our paper can be accepted for publication on SciPost Physics.

Best regards,

The authors

Reply to Referee #1

We are grateful to the Referee for her/his effort in assessing the manuscript, which helped us to improve its content. We answer in the following to all the points they raised. We have also introduced all the changes requested by the Referee in the revised version of the manuscript. Therefore, we hope that this new version of our paper can be accepted for publication on SciPost Physics.

Report

Drawing the comparison to plasma orbit theory to describe the dynamics of vortices with massive cores clearly meets the expectation of SciPost to 'Provide a novel and synergetic link between different research areas' and for this reason I believe this article is suitable for publication following revision. It is also evident that there are clear avenues for future research stemming from the results presented in this article, for example, what do the perturbed dynamics of a necklace of 'pairs' of massive vortices look like? How do the dynamics change when the initial position of only a single vortex in the necklace is perturbed? As well as other avenues for future work discussed by the authors in the article.

We thank the Referee for the positive and constructive report. We are glad to see that they appreciated the novelty of the plasma orbit theory and the experimental applications. We are also grateful for the new future perspectives suggested by the Referee that can be developed in future works.

Weaknesses

We hope that the changes brought to the work, as kindly suggested by the Referee, have fixed the weaknesses of the original version. Here below we briefly comment and summarize the improvements for each weak point.

(1) While the results are interesting, the article is dense to read and it is difficult to follow the derivations and results presented.

We improved the readability of the article, as explained in the Reply to Point (1) of the Requested changes.

(2) It appears that most of the theoretical machinery (massive point vortex models) and some of the results have already been derived in previous work and the novelty of the article lies in drawing the analogy to plasma orbit theory.

In the revised version we further clarified the novelties associated to the ring geometry, both in terms of non-trivial topological properties and experimental realizations.

(3) The article would benefit from including a discussion of the results using physical intuition (*i.e.* interaction between point vortices and image vortices, comparison to point vortex in a channel or around a hard circular boundary) to explain and help the reader understand why the results make sense.

The Referee can find a detailed answer in the Reply to Point (3) of the Requested changes.

(4) The language used around describing the results and the conditions for dynamics with radial oscillations, 'plasma orbit' and epitrochoid curves could be improved. For example, from the abstract, one could understand that the combination of radial oscillations on top of the usual uniform precession trajectories are equilibrium dynamics of massive vortices. However reading the article it becomes clear that these sorts of trajectories arise when the initial position of the massive vortices are perturbed, and so (please correct me if I am misunderstanding) would better be described as excited state trajectories of massive vortices.

As explained in the Reply to Point (2) of the Requested changes, the combination of radial oscillations on top of the usual uniform precession can be considered as an excited state trajectory since it has a larger total

conserved energy compared to the simple uniform precession: in any case, these are *stable* excited states since the trajectory is always bound between a maximum and a minimum radial coordinate. We modified the abstract following the suggestion in Point (9), deleting the ambiguous term "regular motion".
In our opinion, we managed to provide a neat explanation of the peculiar *epitrochoidal* curves described within the *plasma orbit theory*: after being introduced at the end of Sec. 2, these are developed throughout Sec. 3 with a mainly qualitative explanation (see for instance Fig. 5). More quantitative mathematical details can then be found in Appendix C.3.

Requested changes

(1) Considering the points raised earlier, my main suggestion is that the authors try to improve the readability of the article.

We carefully considered the Referee's suggestion and we made efforts to improve the readability of the text. Most of the attention was devoted to the Introduction, in order to provide a clearer presentation of the whole structure of the work, and to Sec. 2, with the main aim of bringing out the physical meaning from the results of the analytical model. In the following, the Referee can find a more detailed list of the new parts introduced in the revised version of the manuscript: we mention also those changes required by the Referee that we think contributed to a more plain and comprehensible paper.
We revised the abstract, getting rid of the source of confusion explained by the Referee in Point (9). In the final part of the Introduction we expanded the outline of the work putting more emphasis on the crucial novelties that characterize the annular geometry and that motivate our work, especially in terms of feasible experimental realizations. The general validity of the *plasma orbit theory* was highlighted and a brief comment about the Appendices was added in order to further clarify the organization of the material.
Several changes were made in Sec. 2 to fulfill various points raised by the Referee, starting from a better explanation of the notation $(\boldsymbol{r}, \{\boldsymbol{r}_j\})$ as asked in Point (4). Sec. 2.1 was expanded with a discussion based on physical intuition according to Point (3): we specified the infinite set of image vortices required by the presence of two borders and we presented some interesting limits for the annular geometry. The physical explanation for the changing sign in the angular velocity and a clarification on the radial displacement [referring to Point (7)] were added in Sec. 2.2.
Considering both the Report and Point (2) of the Requested Changes by the Referee #2, we improved Sec. 4 with a comment about the immiscibility condition for the (experimentally relevant) case of trapped gases and the inclusion of more simulation details in view of a total reproducibility of the results.
Finally, in the Appendices we implemented Point (10) raised by the Referee and we believe this is another valuable step towards a better readability of the paper.

(2) Is it appropriate to understand the trajectories that deviate from circular orbits with uniform angular velocity, such as radial oscillation on top of uniform precession as excited state dynamics?

Yes, that's correct. Indeed, the derivation of the effective potential in Eq. (25) of the manuscript, whose details can be found in Ref. [1], naturally introduces an effective total energy that is a conserved quantity during the vortex dynamics:

$$\frac{1}{2}\tilde{\mu}\dot{r}^2 + V_{\text{eff}}(r) = E = \text{const.} \tag{R.1}$$

In the lowest energy configuration, $E \equiv E_0 = V_{\text{eff}}^{\text{min}}$, there is no radial motion ($\dot{r} = 0$) and the dynamics corresponds to a uniform precession with constant angular velocity Ω at a fixed radius r_0 related by the minimum condition $\mathrm{d}V_{\text{eff}}/\mathrm{d}r|_{r_0,\dot{\theta}_0=\Omega} = 0$. The procedure we followed in the manuscript consists in changing the initial radial position (r_{in}) and angular velocity in order to keep the angular momentum ℓ fixed, hence the same $V_{\text{eff}}(r)$ (that depends on ℓ and μ). The total conserved energy of this new dynamical configuration is easily evaluated at either one of the two classical turning points (where $\dot{r} = 0$), giving $E = V_{\text{eff}}(r_{in}) > E_0$: therefore, all trajectories that deviate from circular orbits with uniform angular velocity can be understood as excited state dynamics since they are characterized by a higher (conserved) total energy.
Despite being technically correct, we preferred to avoid the terminology of "excited state dynamics" since

the latter is not usual in classical mechanics.
We added a sentence below Eq. (28) of the revised version of the manuscript to better clarify this point.

(3) Where it makes sense, include a discussion of dynamics using physical intuition - ***i.e.*** **interaction between point vortices and image vortices, comparison to point vortex in a channel or around a hard circular boundary. Relating to this, what is the reason behind the angular velocity in figure 2(a) changing sign with the radius of the circular orbit? Can you also explain the changing sign in angular velocities in later figures?** ***i.e.*** **8(a) and 9(b).**

We thank the Referee for raising this interesting point because it gave us the opportunity to provide further physical insight on the dynamics of massive vortices on a planar annulus. To unveil the relationship between the geometry of the system and the interaction between physical and image vortices, we addressed three particular limits for the ring geometry. This reasoning stimulated the detailed analysis that we present below. In the revised version of the manuscript, instead, we limited ourselves to adding a simpler discussion based on physical intuition.

The presence of two boundaries requires an infinite set of images, as it is known from electrostatics [2]. Given a positive vortex at position r_0 inside an annulus with radii $R_1 < R_2$, the image vortices are arranged with alternating sign along the same radial direction at positions labelled by the integer $m \in \mathbb{Z}$ [3]:

$$\text{positive:} \qquad r_+^{(m)} = r_0 \left(\frac{R_2}{R_1}\right)^{2m}, \qquad\qquad \text{negative:} \qquad r_-^{(m)} = \frac{R_2^2}{r_0}\left(\frac{R_2}{R_1}\right)^{2m} \tag{R.2}$$

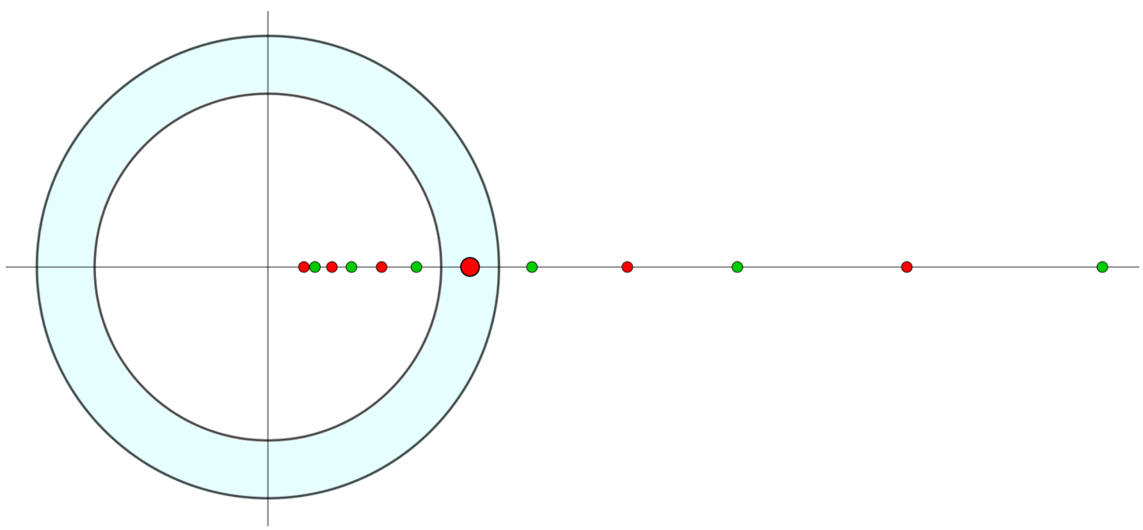

Figure R.1: Schematic representation of the infinite set of image vortices required in the annular geometry. The first pairs for $m \in [-3, 2]$ are explicitly shown. The positive physical vortex is the red dot inside the blue shaded area and it has a bigger size for sake of visibility. The color of the dots is associated to the charge of each vortex that can be either $+1$ (red) or -1 (green). Only the closest image vortices are shown, beyond both boundaries.

A pictorial representation of the first images beyond both the borders (corresponding to $m \in [-3, 2]$) can be found in Fig. R.1, where the physical vortex inside the annular region is highlighted with a larger size. The different colors represent the charge of each vortex, which can be either $+1$ (red) or -1 (green).
We discuss three particular limits:

- $R_1 \ll R_2$, with $\mathfrak{n}_1 = 0$: the annulus reduces to a disk of radius R_2.
From Eq. (R.2) it is easy to see that both $r_+^{(m)}, r_-^{(m)} \to \infty$ for $m > 0$, while $r_+^{(m)}, r_-^{(m)} \to 0$ for $m < 0$. As shown in Fig. R.2(a), all the pairs of image vortices with $m \neq 0$ annihilate (at the origin or at infinity), the only two finite contributions remaining are the ones corresponding to $m = 0$, *i.e.* the positive physical vortex at r_0 and the negative image vortex at position $r_0' = R_2^2/r_0$. This is exactly the well known case of a vortex inside a circular trap [1], where a single image vortex of opposite charge is required. Notice that it was already derived in Ref. [4] that in the limit $R_1 \to 0$ one recovers the results for a disk with radius R_2.

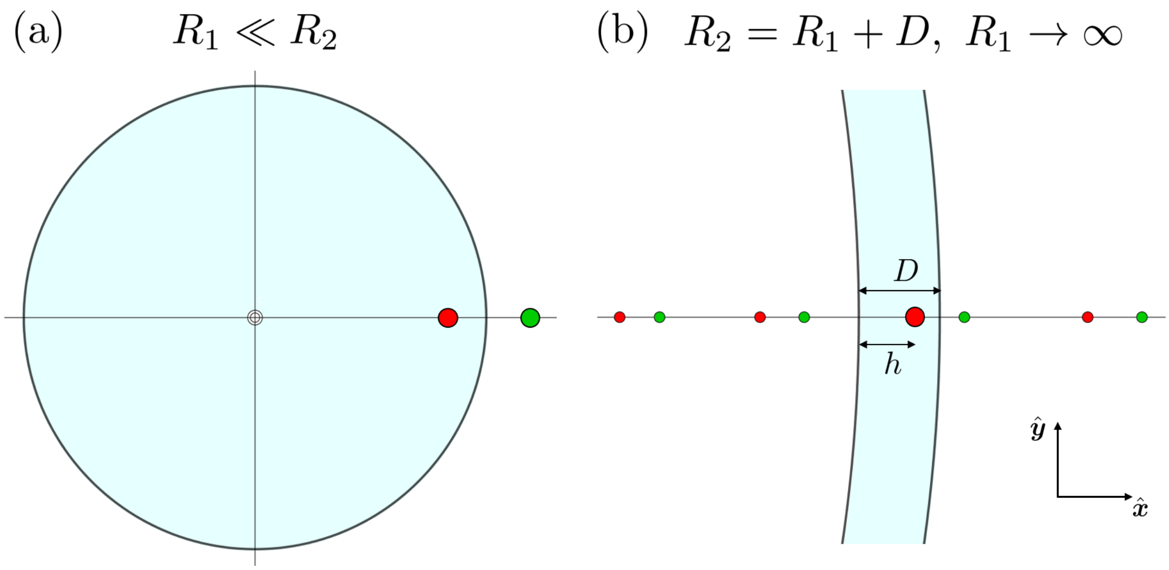

Figure R.2: Two limits for the position of the inner boundary R_1. (a) When $R_1 \ll R_2$ and $\mathfrak{n}_1 = 0$, the annulus reduces to a disk of radius R_2 and all the image vortices annihilate except the first one beyond the outer boundary: this has negative charge and is located at $\boldsymbol{r}_0' = (R_2/r_0)^2 \boldsymbol{r}_0$, as expected for the case of a hard circular boundary. (b) In the limit $R_1 \to \infty$, with $R_2 = R_1 + D$, the curvature becomes irrelevant and the annulus approaches a rectilinear channel of width D.

- $R_1 \to \infty$, with $R_2 - R_1 = D$
Let us consider a very large inner radius, keeping a constant width D of the annulus. As R_1 increases, the curvature of the annulus becomes irrelevant and the system is expected to reduce to an infinitely long but transversely confined channel, or slab, with width D: this geometry is shown in Fig. R.2(b). To better understand this limit, let us denote with h the distance of the physical vortex from the inner border, such that:

$$r_0 = R_1 \left(1 + \frac{h}{R_1}\right), \qquad R_2 = R_1 \left(1 + \frac{D}{R_1}\right) \tag{R.3}$$

Substituting inside Eq. (R.2) and retaining up to linear terms in h/R_1 and D/R_1, one gets the following positions for the infinite set of vortices:

$$r_+^{(m)} \simeq R_1 + h + 2mD, \qquad r_-^{(m)} \simeq R_1 - h + 2(1+m)D = r_+^{(m)} + 2(D-h) \tag{R.4}$$

A given vortex at $r_+^{(m)}$ is at distance $2(D-h)$ from the anti-vortex on the right, $r_-^{(m)}$, and at distance $2h$ from the anti-vortex on the left, $r_-^{(m-1)}$. Moving to a Cartesian reference frame where the y-axis is parallel to the left boundary and the x-axis passing through the vortex, the positions of the positive and negative vortices are:

$$x_+^{(m)} = h + 2Dm, \qquad x_-^{(m)} = 2D - h + 2Dm, \qquad y_+^{(m)} = y_-^{(m)} = 0 \tag{R.5}$$

These positions (and the $2D$ periodicity) are compatible with the results presented in Ref. [5]: in particular, we refer to their expression for the complex potential in Eq. (4) and to their schematic representation of the channel geometry in Fig. 1(a) that is compatible with our Fig. R.2(b).

We recall that the interaction between vortices on a planar geometry is given by a 2D Coulomb-like force scaling with the inverse of the distance. Among the infinite image vortices, as shown in Fig. R.2(b), the first one (with opposite sign) beyond each of the two borders provides the most relevant contribution to the interaction. Following the electromagnetic analogy carefully explained in the text, for each of the two vortex and anti-vortex pair we can identify an electric field along the x-direction pointing from the physical vortex (positive charge) to the image one (negative charge): the total effective electric field is the sum of these two contributions. Together with the effective magnetic field $\boldsymbol{B} \propto -\hat{\boldsymbol{z}}$, the electric field is responsible for a uniform translation of the vortex along the y-direction with drift velocity $\boldsymbol{v}_d \propto \boldsymbol{E} \times \boldsymbol{B}$. When $0 < h < D/2$, the electric field is $\boldsymbol{E} \propto -\hat{\boldsymbol{x}}$ and the vortex moves downwards ($\boldsymbol{v}_D \propto -\hat{\boldsymbol{y}}$). When $D/2 < h < D$, instead, $\boldsymbol{E} \propto +\hat{\boldsymbol{x}}$ and the vortex moves upwards ($\boldsymbol{v}_D \propto +\hat{\boldsymbol{y}}$). Finally, when the vortex is at the centre of the channel ($h = D/2$) one has a linear chain of infinite equidistant charges with alternating sign. The physical vortex inside the slab doesn't feel any net effect from the presence of the image ones, because they perfectly cancel in pairs: as a consequence, it doesn't move. All these last comments perfectly fit the analytical expression for the vortex velocity in Eq. (16) of Ref. [5] that correctly accounts for the contribution of all the other infinite image vortices.

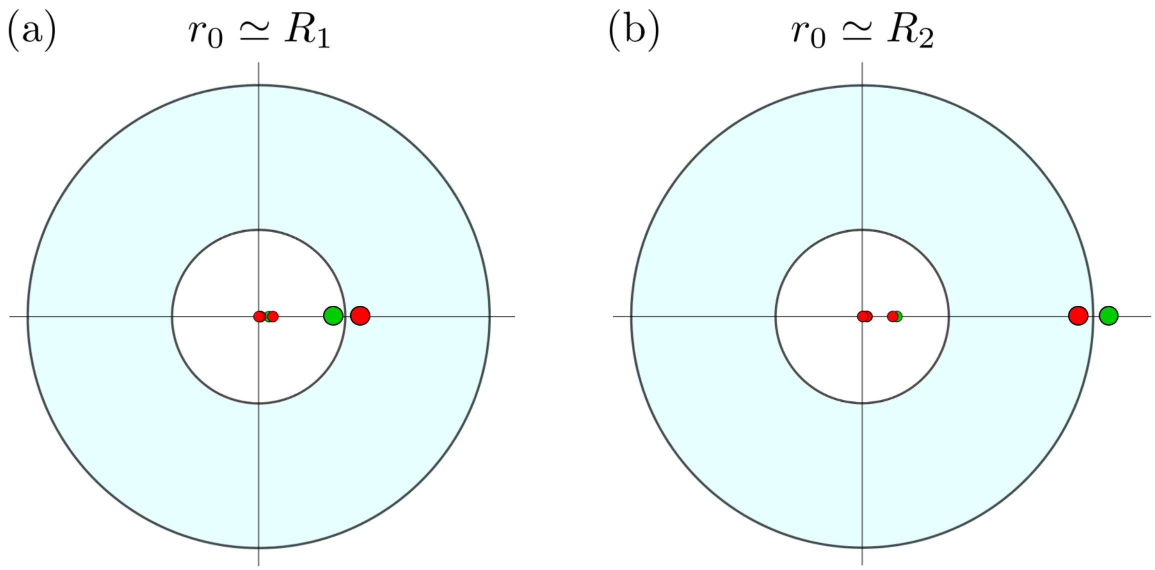

Figure R.3: When the vortex gets close to the inner (a) or outer (b) boundary, the dominant effect is the interaction with the closest image with opposite sign. This results in opposite signs for the angular velocity of the uniform precession.

- $r_0 \simeq R_1$, or $r_0 \simeq R_2$: the vortex gets close to one of the edges.
  Fig. R.3 shows the two situations where the physical vortex inside the annular region approaches the inner (a) or outer boundary (b). One can see that the first image vortex (with opposite sign) beyond the border gets closer, thus providing the most relevant contribution to the interaction. We can identify an effective electric field along the radial direction pointing from the physical vortex (positive charge) to the image one (negative charge). Together with the effective magnetic field $\boldsymbol{B} \propto -\hat{\boldsymbol{z}}$, the electric

field is responsible for the uniform precession of the vortex with tangential velocity $\boldsymbol{v}_\theta \propto \boldsymbol{E}\times\boldsymbol{B}$. Using polar coordinates $(\hat{\boldsymbol{r}}, \hat{\boldsymbol{\theta}})$, the reason why the angular velocity in Fig. 2(a) changes sign appears now clear:

- close to the inner boundary R_1, as in Fig. R.3(a), $\boldsymbol{E} \propto -\hat{\boldsymbol{r}}$ so that $\boldsymbol{v}_\theta \propto -\hat{\boldsymbol{\theta}}$ and the vortex performs a clockwise rotation (negative angular velocity);
- close to the outer boundary R_2, as in Fig. R.3(b), $\boldsymbol{E} \propto \hat{\boldsymbol{r}}$ and $\boldsymbol{v}_\theta \propto \hat{\boldsymbol{\theta}}$ is compatible with a counterclockwise rotation (positive angular velocity).

We added a summarized version of the discussion of these three limiting cases at the end of Sec. 2.1 of the revised version of the manuscript, as well as an explanation for the changing sign of the angular velocity just below Eq. (24) in Sec. 2.2. The changing sign of angular velocities in later Figs. 8(a) and 9(b) is motivated by the same physical discussion that has just been developed, so we think that no more comments are required in the work.
An additional comment for the limit $R_1 \to 0$ can be found at the end of Appendix D.

(4) The notation $(\boldsymbol{r}, \{\boldsymbol{r_j}\})$ is confusing. Please explain this in the text.

This notation is defined in Sec. 2.1 of the manuscript, where we introduce the trial wave functions ψ_a and ψ_b of the two components. The reason behind our choice is to highlight that the trial wave functions are defined over the 2D space $\boldsymbol{r} \in \mathbb{R}^2$ and they also carry a parametric dependence on the coordinates of the N_v vortices inside the condensate (here $\{\boldsymbol{r}_j\}$ is a short-hand notation for $\{\boldsymbol{r}_j\}_{j=1,\dots,N_v}$). The spatial variables $\boldsymbol{r}$ are integrated out by the time-dependent variational Lagrangian method, so that the resulting Lagrangian is a function of the coordinates of the vortices only. We added a comment at the beginning of Sec. 2.1 to better clarify this point.

(5) Assumption of a cut-off at the vortex core - does it break at some point with increasing mass?

The assumption of a cut-off at the vortex core is mentioned in Sec. 2 of the main text, between Eqs. (8) and (9), but it only explicitly enters Appendix B.2 where the potential energy functional $\Delta\mathcal{E}_a$ is derived. We consider the model of a circular vortex core of radius a_c that allows to cure UV divergences in the integrals required by the time-dependent variational Lagrangian method. Notice that we changed the notation for the core radius from a to a_c in order to avoid any confusion with the first component of the mixture, always labelled as species a. The dependence of the final result in Eq. (63) of the paper on the cut-off a_c is reduced to an additive constant that is irrelevant for the equations of motion: the assumption of a cut-off at the vortex core does not have any physical relevance in the vortex dynamics that we studied in this paper. For this reason we did not comment about it in the main text of our work.
For the sake of completeness, we note that the presence of a finite core mass generally enhances the core-size: an interesting analysis about how the characteristic size of the vortex core gets modified by the mass can be found in Sec. VI of Ref. [6].

(6) How would the dynamics change if only the initial position of the massive core was shifted but the vortex was not? Would similar dynamics occur?

One of the main assumptions of our point-vortex model is that the centre of the vortex core (*i.e.*, the phase singularity of the wave function ψ_a) and the mass (*i.e.*, the centre of the Gaussian wave function ψ_b) are described by the same coordinates. From a physical point of view, the more *immiscible* is the mixture ($g_{ab} > \sqrt{g_a g_b}$), the more valid is the assumption: the massive b-component is “locked” inside the cores of species a and the relative degrees of freedom can be safely neglected. We would like to point out that this assumption can be relaxed and the possible relative motion between a vortex and its massive core will be described in [A. Bellettini, A. Richaud, and V. Penna], which is going to be published soon.

(7) How do you define a small displacement and what is the appropriate length-scale to compare to? Vortex core size? The displacement seems quite large in some cases.

The initial displacement δ has to be compared to the radius of the uniform circular orbit r_0. The condition of small displacement, then, is given by $\delta \ll r_0$.
The vortex core size is instead taken to be zero in the point-vortex model, and as such it may not provide an appropriate length scale for comparing with δ.
In the final paragraph of Sec. 2 of the new draft we specified that the displacement has to be small compared to the radius of the uniform precession.

(8) In figure 3(a) there is no blue shaded region (which is referred to in the text). I assume you mean the brownish region to the right of the blue line.

We thank the Referee for bringing this detail to our attention. We substituted *blue* with *light brown* both in the caption of Fig. 3(a) and in the part of the text where we referred to that region.

(9) On first reading the paper, I found this sentence ambiguous:
'This regular motion' becomes unstable beyond a critical vortex mass.
By 'this regular motion' are the authors referring to the radial oscillations around the annulus?

With the term *regular motion* we were referring to the one made of small radial oscillations on top of a uniform precession. We improved this sentence in the abstract using *oscillatory motion* and mentioning the effect of the instability, *i.e.* the expulsion of the vortices at the edges. This should have clarified the ambiguity.

(10) For ease of readability please include the final equation derived in appendices also in the appendix in addition to referring back to the body of the article.

Following the Referee's suggestion, we modified the Appendices by including those final equations that were previously only referred back to the body of the article. The location of these changes in the revised version of the manuscript are: Appendix B.2, end of the first paragraph of Appendix C, Appendix C.2 and Appendix D.1.

Reply to Referee #2

We are grateful to the Referee for her/his effort in assessing the manuscript, which helped us to improve its content. We answer in the following to all the points they raised. We have also introduced all the changes requested by the Referee in the revised version of the manuscript. Therefore, we hope that this new version of our paper can be accepted for publication on SciPost Physics.

<u>**Report**</u>
The paper is of high scientific quality, and there is no doubt that this work comprehensively uncovers the physics of the orbits of vortices with an in-filling component, within the potential considered. Looking to the journal's acceptance criteria, of the 6 mandatory requirements there is work required to aid the reader in understanding the work presented (point 1) and more simulation details should be added such that the reader could reproduce the results (point 5). Regarding the expected criteria, the work does provide a novel and synergetic link between different research areas, by linking the observations to plasma orbit theory. Ultimately, I believe the work should be accepted after revisions. Crucially, a paragraph in the introduction needs to properly motivate how this system differs from that covered in Refs. [20,21,30], and what novelty does the inclusion of this inner ring boundary bring. Would the results for the plasma orbit theory worked just as well for the disk condensate case?

We thank the Referee for the positive and constructive report: the quality of our work indeed benefited from his/her specific requests and suggestions.
Point 1 of the journal's acceptance criteria says that the paper must "be written in a clear and intelligible way, free of unnecessary jargon, ambiguities and misrepresentations": thanks to the various remarks raised by the two Referees, we think we have now fully achieved the task [we refer to the Reply to Point (1) of the Requested changes by Referee #1].
As far as point 5 is concerned, according to which the paper must "provide (directly in appendices, or via links to external repositories) all reproducibility-enabling resources: explicit details of experimental protocols, datasets and processing methods, or processed data and code snippets used to produce figures, etc.", more simulations details have been added in Sec. 4 of the revised version of the manuscript.
The novelties brought by the inclusion of the inner ring boundary can be mainly identified with the persistent current which may circulate on it (with quantized circulation controlled by the integer $\mathfrak{n}_1$) and the infinite set of image vortices. Moreover, as pointed out in the Conclusions, the annular geometry is interesting due to its topological equivalence with a cylinder of finite length and the possibility of implementing the hydrodynamic analog of the Laughlin pumping. We added a few comments in the last paragraph of the Introduction to motivate how our system differs from the circular trap already studied in previous works and to clarify that the results for the *plasma orbit theory* are general and valid for an arbitrary planar geometry.

<u>**Weaknesses**</u>
We hope that the changes brought to the work, as kindly suggested by the Referee, have fixed the weaknesses of the original version. Here below we briefly comment and summarize the improvements for each weak point.

(1) The paper is an extension of Refs. [20,21,30], in a ring rather than a disk, and the appearance of *epitrochoidal* orbits is expected.

We better unveiled the analogies and differences between the ring and disk geometries by introducing comments and discussions at the end of the Introduction and of Sec. 2 [see the Reply to Point (1) of the Requested changes by Referee #1 for a more detailed list of these changes]. On the one hand, we put emphasis on the new physics introduced by the inner ring: the need for an infinite set of image vortices, the possibility of a finite persistent current $\mathfrak{n}_1$ and the same non-trivial topology of a cylindrical surface of finite length. On the other hand, we thoroughly demonstrated how the results for a disk can be recovered in the limit $R_1 \to 0$.

(2) Involving three methods in one paper means that there's a lot of notation to understand and digest.

We made a great effort to improve the readability of the work by shedding light on the physical motivations of the various results and presenting only the mathematics strictly required. We also think the Appendices provide all the necessary information for the reader who wanted to rederive the analytical results.

(3) Some overlapping notation ("a" and "b" are used multiple times in different contexts)

We thank the Referee for this comment: after a careful reading of the manuscript, we found two cases of overlapping notation where a and b have a different meaning than the label of the two species the mixture is made of. In the derivation of the potential energy functional in Appendix B.2 we had used a as the cut-off representing the radius of the circular vortex core: it is now renamed a_c in the new version of the work. The second possible case of overlapping notation could be found in Appendix C.3 where a and b denote the radii of the two circles whose motion describes *epitrochoidal* trajectories. We decided not to introduce any change there since there is no mention to the two species that could give rise to ambiguities.

Requested changes

(1) How appropriate is the quasi-2D model for the parameters chosen? With the thickness taken, d_z, do you satisfy the condition $\mu << \hbar\omega_z$?

The relation between the effective thickness (d_z) and the trapping frequency along the z direction (ω_z) [7, 8] allows to write the harmonic energy as:

$$\hbar\omega_z = \frac{2\pi\hbar^2}{m d_z^2} \tag{R.6}$$

Consider the a-component, which is spread over the whole annular region. Its wave function ψ_a satisfies the stationary GP equation

$$\left[-\frac{\hbar^2\nabla^2}{2m_a} + V_{\rm ext}(\boldsymbol{r}) + \frac{g_a}{d_z}\left|\psi_a(\boldsymbol{r})\right|^2\right]\psi_a(\boldsymbol{r}) = \mu_a\psi_a(\boldsymbol{r}) \tag{R.7}$$

where the external box-like potential $V_{\rm eff}(\boldsymbol{r})$ is equal to zero inside the annular region $R_1 < r < R_2$. The a-condensate can be treated within the Thomas-Fermi approximation, therefore one can neglect the kinetic energy contribution and get the number density:

$$n_a(\boldsymbol{r}) = \frac{d_z}{g_a}\left(\mu_a - V_{\rm ext}(\boldsymbol{r})\right) \tag{R.8}$$

Due to the shape of the potential, the density is different from zero only inside the annular region $R_1 < r < R_2$ and the chemical potential is obtained as:

$$N_a\mu_a = \int_{ann} d^2r\,\frac{g_a}{d_z}n_a^2(\boldsymbol{r}) \qquad \rightarrow \qquad \mu_a = \frac{g_a N_a}{\pi\left(R_2^2 - R_1^2\right)d_z} \tag{R.9}$$

Expressing the interaction constant in terms of the s-wave scattering length a_a, $g_a = 4\pi\hbar^2 a_a/m_a$, the ratio between Eqs. (R.9) and (R.6) reads:

$$\frac{\mu_a}{\hbar\omega_z} = \frac{2N_a a_a d_z}{\pi\left(R_2^2 - R_1^2\right)} \tag{R.10}$$

If we denote with $\overline{R}$ the length scale representing the spatial extension of the condensate (for the ring geometry we can identify $\overline{R} = R_2 - R_1$), the two contributions to the total energy can be estimated as:

$$E_{kin} = \left\langle -\frac{\hbar^2\nabla^2}{2m_a}\right\rangle \simeq \frac{\hbar^2}{2m_a\overline{R}^2}, \qquad E_{int} = \left\langle \frac{g_a}{2d_z}\left|\psi_a\right|^2\right\rangle \simeq \frac{g_a}{2d_z}\frac{N_a}{\overline{R}^2} \tag{R.11}$$

In the Thomas-Fermi regime, the kinetic energy associated with the density variation becomes negligible compared to the interaction energy. In terms of the microscopic parameters of the model, the validity condition of the Thomas-Fermi approximation is the following:

$$\frac{E_{int}}{E_{kin}} = \frac{m_a g_a N_a}{\hbar^2 d_z} \propto \frac{N_a a_a}{d_z} \gg 1 \tag{R.12}$$

For the numerical GPE simulations presented in the text, we used the following parameters for species a

$$N_a = 5\times 10^4, \qquad a_a = 2.75\times 10^{-3}\,\mu\mathrm{m}, \qquad d_z = 2\,\mu\mathrm{m}, \qquad R_1 = 5.0\,\mu\mathrm{m}, \qquad R_2 = 50.0\,\mu\mathrm{m} \tag{R.13}$$

from which we obtain

$$\frac{\mu_a}{\hbar\omega_z} \simeq 0.07 \ll 1 \qquad\qquad \frac{N_a a_a}{d_z} \simeq 69 \gg 1 \tag{R.14}$$

These estimates confirm that both the *quasi*-2D model and the Thomas-Fermi approximation for the a-condensate are appropriate: we wrote it explicitly in Sec. 4 when discussing about the parameters chosen for the numerical simulations.

(2) The immiscibility condition stated is only exactly true when the atom numbers between the components are equal. Though you are clearly in the immiscible regime, the text should be modified and a citation to the work of K. L. Lee et al., Phys Rev A 94, 013602 (2016) should be added.

The stability condition for a homogeneous gas of two components is discussed, for example, in Sec. 12.1.1 of Ref. [9]. The *miscible* regime is described by Eq. (12.14) that, with our notation, can be cast into:

$$g_a > 0, \qquad g_b > 0, \qquad g_a g_b > g_{ab}^2 \tag{R.15}$$

In our two-component mixture, the confining potential is composed of hard-walls and the majority component is in the Thomas-Fermi regime, therefore the species a is effectively uniform apart from those regions around the vortices. Nevertheless, the latter constitute preformed potential wells for the component-b bosons which can thus localize therein for values of g_{ab} not necessarily larger than the well-known critical quantity $\sqrt{g_a g_b}$. As a consequence, the requirement $g_{ab} > \sqrt{g_a g_b}$ is a sufficient condition for the stability of massive vortices in a binary Bose mixture. We have better clarified this last point in the text.
Nonetheless, we agree with the Referee that a discussion of the *immiscibility* condition for trapped gases is missing: we added a comment in the revised version of the manuscript, introducing a citation to the proposed work.

(3) I think the equations and model may be a little easier to follow by simply deleting all terms with $\mathfrak{n}_1$ (the persistent current). In this work, you always consider $\mathfrak{n}_1 = 0$, and the 91 (!) equations are already tough enough as it is.

We recognize that our work is quite technical and, as a consequence, we made a great effort to improve its general readability. A lot of time was devoted, during the writing of the first version of the manuscript, to the choice of which equations to present: we are aware of their huge number, but we do believe we have found the right compromise that allows the reader to understand the various passages without neither skipping important details, nor getting stuck in the mathematics. On the contrary, we do not believe that the deletion of all the terms $\mathfrak{n}_1$ could actually make the model sensibly easier to follow. We would like to explain to the Referee the two main reasons behind our point:

- $\mathfrak{n}_1$ represents the persistent current along the inner boundary, a peculiar feature of the ring geometry that is related to its topology and that marks one of the main differences with other planar geometries already studied (like the circular trap). It is true that we have always taken $\mathfrak{n}_1 = 0$ in the graphs we showed, but we consider important to leave the explicit dependence of the equations on $\mathfrak{n}_1$, in order to guarantee that our discussion remains as general as possible;

- $\mathfrak{n}_1$ appears inside 6 equations of the main text and 12 equations of the Appendices: in our opinion, no major improvements would be introduced by deleting it.

(4) In the conclusions it is stated that the GP was extensively tested against the point-vortex model, I think in order for this statement to hold true a comparable GP simulation should also be done to match the onset of vortex expulsion from the condensate.

We actually performed numerical GP simulations for the vortex expulsion from the condensate, but we decided not to present them in the work due to issues related to the size of the vortex core. To better clarify this point, we show in Fig. R.4 the results of one of these simulations where we fixed the mass ratio to the critical value $\mu = \mu_{c,2}$. More specifically, the initial conditions match the ones for a uniform precession with radius $r_0 = 30\,\mu\text{m}$ and angular velocity $\dot{\theta}_0 = 1.47\,\text{rad/s}$: with such a r_0 one gets $\mu_{c,2} \simeq 0.25$, hence $N_b \simeq 7500$ (since $N_a \simeq 5 \times 10^4$). The comparison between the numerical trajectory (blue curve) and the analytical prediction from the point-vortex model (orange curve) is presented in Fig. R.4(a): the two solutions display a remarkable agreement up to a certain point where the numerical one seems to bounce back towards the annular region. The size of the vortex core is the reason for this behaviour, as it can be understood by looking at the density profile of the a-component in Fig. R.4(b): in this situation, indeed, the mass ratio is five times bigger compared to the one analyzed in Fig. 7 of the paper. Thus the numerical solution matches the analytical prediction as long as the vortex core does not touch the outer edge of the annulus: when this happens, the finite core size is such that the real vortex is effectively in touch with its own (closest) image, thus violating one of the crucial assumptions of the point-vortex model. We mentioned this at the end of Sec. 4.

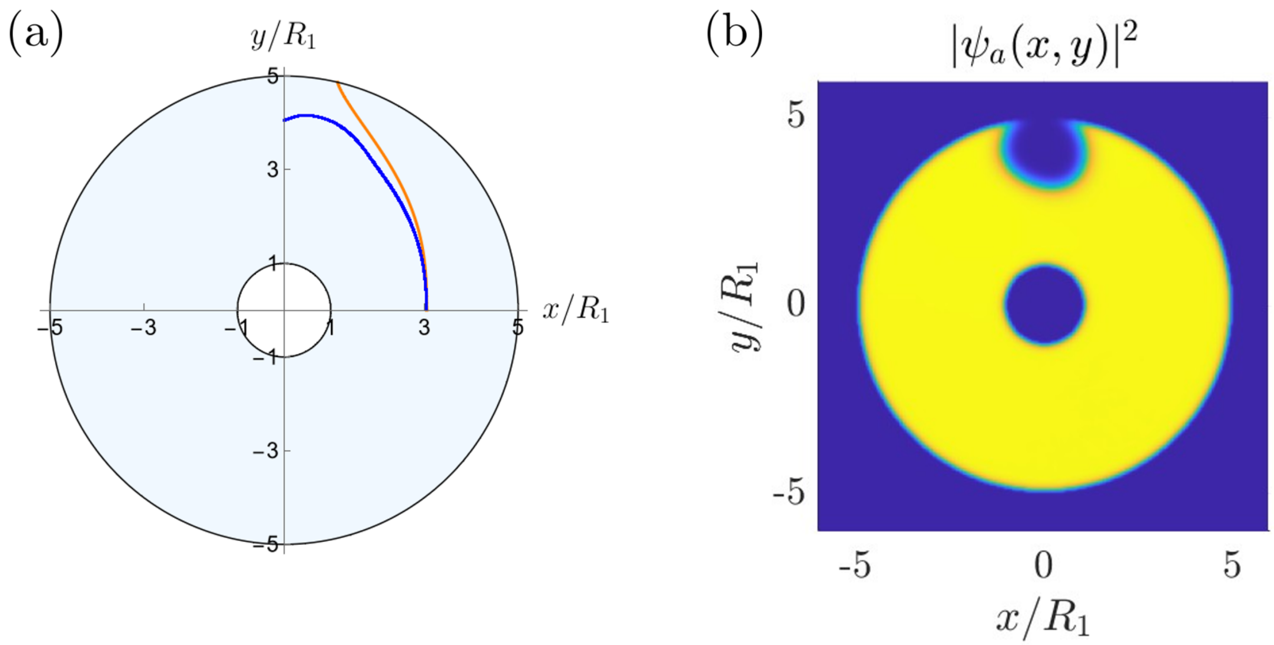

Figure R.4: Numerical simulation of the expulsion of the vortex from the outer boundary when the mass ratio equals the critical value $\mu = \mu_{c,2} \simeq 0.25$. With the same model parameters as for Fig. 6 in the paper, this corresponds to $N_b \simeq 7500$. (a) Comparison between the trajectory obtained with the two-component GP numerical evolution (blue) and the analytical prediction of the massive point-vortex model (orange). (b) Density of the a-component as the vortex hits the outer boundary during the real-time evolution. Blue (yellow) color corresponds to zero (high) values of the density. The (large) finite size of the vortex core is responsible for the deviation of the numerical trajectory from the analytical one.

1 References

[1] A. Richaud, V. Penna and A. L. Fetter, *Dynamics of massive point vortices in a binary mixture of Bose-Einstein condensates*, Phys. Rev. A **103**, 023311 (2021), doi:10.1103/PhysRevA.103.023311.

[2] H. Lamb, *Hydrodynamics*, chap. 7, Dover, New York, 6th edn. (1945).

[3] A. L. Fetter, *Low-Lying Superfluid States in a Rotating Annulus*, Phys. Rev. **153**, 285 (1967), doi: 10.1103/PhysRev.153.285.

[4] N.-E. Guenther, P. Massignan and A. L. Fetter, *Quantized superfluid vortex dynamics on cylindrical surfaces and planar annuli*, Phys. Rev. A **96**, 063608 (2017), doi:10.1103/PhysRevA.96.063608.

[5] L. A. Toikka and J. Brand, *Asymptotically solvable model for a solitonic vortex in a compressible superfluid*, New Journal of Physics **19**(2), 023029 (2017), doi:10.1088/1367-2630/aa5668.

[6] A. Richaud, V. Penna, R. Mayol and M. Guilleumas, *Vortices with massive cores in a binary mixture of Bose-Einstein condensates*, Phys. Rev. A **101**, 013630 (2020), doi:10.1103/PhysRevA.101.013630.

[7] J. Dalibard, *Fluides quantiques de basse dimension et transition de Kosterlitz-Thouless*, Collège de France, Lecture Series 2016-2017.

[8] L. Salasnich, A. Parola and L. Reatto, *Effective wave equations for the dynamics of cigar-shaped and disk-shaped Bose condensates*, Phys. Rev. A **65**, 043614 (2002), doi:10.1103/PhysRevA.65.043614.

[9] C. J. Pethick and H. Smith, *Bose-Einstein Condensation in Dilute Gases*, Cambridge University Press, Cambridge, 2 edn. (2008).